



Structural Transition in the Isotropic Phase of the C12EO6/H2O Lyotropic Mixture: A Rheological Investigation

Doru Constantin, Eric Freyssingeas, Jean-François Palierne, Patrick Oswald

► To cite this version:

Doru Constantin, Eric Freyssingeas, Jean-François Palierne, Patrick Oswald. Structural Transition in the Isotropic Phase of the C12EO6/H2O Lyotropic Mixture: A Rheological Investigation. *Langmuir*, 2003, 19, pp.2554. 10.1021/la026595o . hal-00015646

HAL Id: hal-00015646

<https://hal.science/hal-00015646>

Submitted on 12 Dec 2005

HAL is a multi-disciplinary open access archive for the deposit and dissemination of scientific research documents, whether they are published or not. The documents may come from teaching and research institutions in France or abroad, or from public or private research centers.

L'archive ouverte pluridisciplinaire **HAL**, est destinée au dépôt et à la diffusion de documents scientifiques de niveau recherche, publiés ou non, émanant des établissements d'enseignement et de recherche français ou étrangers, des laboratoires publics ou privés.

Structural Transition in the Isotropic Phase of the $C_{12}EO_6/H_2O$ Lyotropic Mixture : A Rheological Investigation

D. Constantin*, É. Freyssingeas, J.-F. Palierne and P. Oswald
*Laboratoire de Physique de l'ENS de Lyon,
46 Allée d'Italie, 69364 Lyon Cedex 07, France*

Abstract

We study the structural changes occurring in the isotropic phase of the $C_{12}EO_6/H_2O$ lyotropic mixture (up to 35% surfactant weight concentration) upon increasing the concentration and temperature, from small individual micelles to an entangled network which subsequently becomes connected. High-frequency (up to $\omega = 6 \cdot 10^4$ rad/s) rheological measurements give us access to the viscoelastic relaxation spectrum, which can be well described by the sum of two Maxwell models with very different temperature behaviors : the slower one ($\tau_1 \sim 10^{-4}$ s) is probably due to reptation and its associated viscosity first increases with temperature (micellar growth) and then decreases after reaching a maximum (appearance of connections). The fast mechanism ($\tau_2 \sim 10^{-6}$ s) remains practically unchanged in temperature and can be related to the relaxation of local micellar order, as observed at higher concentration in a previous investigation. This interpretation is confirmed by additional measurements in aqueous mixtures of the related surfactant $C_{12}EO_8$ (which forms smaller micelles), where only the fast mechanism –related to local order– is detected.

PACS : 61.30.St, 82.70.Uv, 83.80.Qr

1 Introduction

The isotropic phase of the binary system $C_{12}EO_6/H_2O$, as well as those formed by similar non-ionic surfactant molecules, have been studied for more than twenty years; in the beginning, research focused on the structure at low surfactant concentration, especially on the temperature evolution of micellar size and shape. It is now well established that the micelles have a general tendency of increasing in size and becoming anisotropic (cylindrical) with increasing temperature and concentration (see [1] and references therein). It

*Author for correspondence. Present address : Institut für Röntgenphysik, Geiststraße 11, 37073 Göttingen. E-mail : dconsta@ens-lyon.fr; Tel : +49-551 39 50 66; Fax : +49-551 39 94 30.

has also been shown that micellar growth strongly depends on the molecular details : it is very important for $C_{12}EO_5$ and $C_{12}EO_6$ but much more modest for $C_{12}EO_8$, which forms short micelles.

When they are not too long, these elongated micelles can be seen as rigid rods, but once they exceed a certain persistence length ℓ_p , they become flexible (estimations for the persistence length of $C_{12}EO_6$ vary from 7 nm [2] to 25 nm [3]). If the micelles are much longer than ℓ_p (“wormlike micelles”), they assume very complex configurations resembling polymers in solution, with the essential difference that the micellar length is not chemically fixed, but rather fluctuates around an equilibrium length depending on the thermodynamical parameters, hence the name of “living polymers”. Above an overlap concentration c_c , the micelles begin to touch and become entangled. A quantitative estimate of the curve $c_c(T)$ for the $C_{12}EO_6/H_2O$ system was given in reference [3].

The rheology of entangled polymers is well established [4, 5], and its concepts were recently applied to wormlike micellar systems [6, 7, 8], taking into account the dynamical nature of the micellar length distribution (see [9] for a review). This model was successfully used to describe the rheological behavior of micellar solutions of ionic surfactants [10].

Another interesting property of wormlike micelles is their tendency of interconnecting under certain conditions (concentration, temperature or -in ionic systems- counterion concentration). Such behavior, first found in ternary systems [11, 12], was subsequently observed in a very wide range of binary mixtures of single-tail non-ionic [13, 14, 15, 16, 17, 18] or double-tail zwitterionic [19, 20] surfactants, as well as in pseudo-binary systems (ionic surfactant + brine) [21, 22, 23, 24, 25, 26, 27, 28].

Structurally, connected and entangled systems only differ on a very small scale, which makes them difficult to tell apart using static techniques. Furthermore, the microscopic structure of the connections is far from being elucidated (see [29] and references therein). Indirect techniques must then be employed; for instance, the minimum in surfactant self-diffusion coefficient as a function of the concentration appearing in a wide variety of systems was often explained by the appearance of connections [14]. However, it was shown [30] that this behavior could also originate in the competition between two different mechanisms : diffusion of the micelle itself and diffusion of the surfactant molecule on the micelle.

On the other hand, connections can have a dramatic effect on the *dynamical* properties of wormlike micellar systems. Contrary to connected polymer systems, where the reticulation points (permanent chemical cross-links) slow down the dynamics, connections between entangled micelles can actually facilitate relaxation and render the system more fluid. This aspect prompted a systematic study of the connectivity in micellar solutions : several experiments [22, 23, 31] showed that, in ionic surfactant systems, the viscosity decreases on increasing the salt concentration. They were followed by theoretical works on the conditions of connection formation [32] and their influence on the dynamics of the phase [33]. The theory was then employed to qualitatively characterize the appearance of connections [24, 25, 27]. Briefly, branching points allow the surfactant to “flow” more easily across the micellar network, thus increasing the curvilinear diffusion constant of a micelle D_c . As the terminal relaxation time in entangled systems is the reptation time $\tau_R = L^2/D_c$, this amounts (from the dynamical point of view) to replacing the average length of a micelle by the average distance between branching points along a micelle

[9]. When the latter becomes of the order of the entanglement length, the network is termed “saturated” [32]; in this case, the concept of reptation is no longer valid and other relaxation mechanisms, such as those related to the local order, can become dominant [34].

The purpose of this article is to study the structural changes that occur in the isotropic phase of an aqueous solution of non-ionic surfactant upon increasing the concentration or the temperature, from small individual micelles to an entangled network which then becomes connected. We achieve this by relating the viscoelastic relaxation mechanisms to the structural features and by monitoring their evolution with concentration and temperature.

We employ high-frequency rheology to study the isotropic phase in the $C_{12}EO_6/H_2O$ lyotropic mixture, where $C_{12}EO_6$ is the non-ionic surfactant hexa-ethylene glycol mono-n-dodecyl-ether, or $CH_3(CH_2)_{11}(OCH_2CH_2)_6OH$ (for the phase diagram see [35]). Its dynamic behavior has already been investigated by measuring the shear viscosity [36, 37], sound velocity and ultrasonic absorption [37], as well as NMR relaxation rates [38], all pointing to the presence of wormlike micelles (at least above 10 % surfactant concentration by weight [37]). In previous experiments [39, 40] we have shown that, for 50 % wt surfactant concentration, above the hexagonal mesophase, the isotropic phase has a structure consisting of surfactant cylinders that locally preserve the hexagonal order over a distance d varying from about 40 nm at 40 °C to 25 nm at 60 °C. Local order is equally evidenced at lower concentration (down to about 20%) by SANS measurements [41] (let us mention that in some systems local order can appear at very low concentrations, as shown by Kékicheff *et al.* [42]). Between the cylinders there is a large number of thermally activated connections (with an estimated density $n \sim 10^6 \mu m^{-3}$) [40]. Investigating the system at lower concentration, over a wide temperature range, allows us to describe its evolution from small individual micelles to a completely connected network.

For comparison, we also study aqueous solutions of the related surfactant $C_{12}EO_8$, which is known to form smaller micelles [1]. The difference in rheological behavior between the two systems is discussed in terms of the structure.

2 Materials and Methods

The surfactants were purchased from Nikko Chemicals Ltd. and used without further purification. We used ultrapure water ($\rho = 18 M\Omega cm$) from the in-house ELGA system for the $C_{12}EO_6/H_2O$ system. The $C_{12}EO_8$, on the other hand, was mixed with D_2O , as the samples were also used for neutron scattering experiments. The samples were prepared by weighing the components directly into the vials. The mixtures were carefully homogenized by repeatedly heating, stirring and centrifuging and then allowed to equilibrate at room temperature over a few days.

Rheology measurements were performed in a piezorheometer, the principle of which has been described in reference [43] : the liquid sample of thickness 40 or 60 μm is contained between two glass plates mounted on piezoelectric ceramics. One of the plates is made to oscillate vertically with an amplitude of about 1 nm by applying a sine wave to the ceramic. This movement induces a squeezing flow in the sample and the stress

transmitted to the second plate is measured by the other piezoelectric element. The shear is extremely small : $\gamma \leq 2 \cdot 10^{-3}$, so the sample structure is not altered by the flow. The setup allows us to measure the storage (G') and loss (G'') shear moduli for frequencies ranging from 1 to $6 \cdot 10^4$ rad/s with five points per frequency decade. The maximum shear rate is thus $\dot{\gamma} \sim 120$ rad/s, much lower than the characteristic relaxation times (see section 4). The entire setup is temperature regulated within 0.05°C and hermetically sealed to avoid evaporation.

3 Theoretical Considerations

The main relaxation process in entangled polymer solutions is reptation, by which the chain gradually disengages from its initial deformed environment (“tube”) and adopts a stress-free configuration. The typical reptation time is given by : $\tau_{\text{rep}} \simeq L^2/D_c$, with L the chain length and D_c the curvilinear diffusion constant of the micelle in its tube [5], and the shear modulus exhibits exponential decay : $G(t) \sim \exp(-t/\tau_{\text{rep}})$. In the case of wormlike micellar systems, the length distribution $c(L)$ must be taken into account and the resulting relaxation is highly non-exponential [6] :

$$G(t) \sim \exp \left[- \left(\frac{t}{\tau_{\text{rep}}} \right)^{1/4} \right], \quad (1)$$

where τ_{rep} is now given by :

$$\tau_{\text{rep}} = \frac{L_m^2}{D_c}, \quad (2)$$

with L_m the micellar length averaged over $c(L)$.

Another distinctive feature of wormlike micelles is that they can break up and reform, with a typical time τ_{br} . For $\tau_{\text{br}} \gg \tau_{\text{rep}}$, the dynamical response (1) is not affected; in the opposite limit, $\tau_{\text{br}} \ll \tau_{\text{rep}}$, $G(t)$ approaches a single exponential [6], with relaxation time $\tau \simeq \sqrt{\tau_{\text{br}}\tau_{\text{rep}}}$. Besides reptation, which is a process involving the entire chain, additional (local) relaxation modes are present at higher frequency, given by “breathing” (tube length fluctuations) and Rouse dynamics [7, 8].

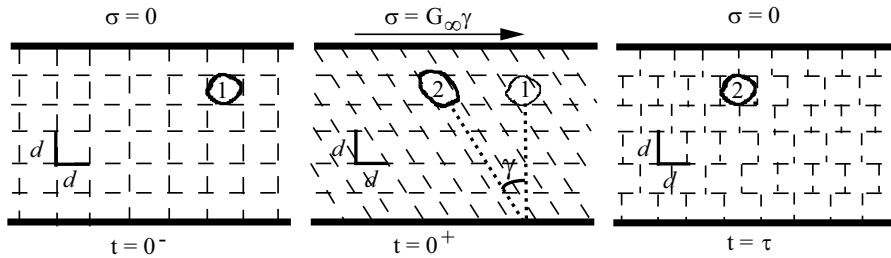


Figure 1: Schematic representation of shear in a material consisting of units of typical size d . One such unit (thick line contour) has been displaced between points 1 and 2. The instantaneous elastic stress is $\sigma = G_\infty \gamma$; it relaxes over a typical time τ given by equation (3).

In a previous paper [34] we showed that in the same mixture at higher concentration, above the hexagonal phase ($c = 50\%$, $T > 40^\circ\text{C}$), the isotropic phase is highly connected

and the viscoelastic response is given by the relaxation of the local micellar order evidenced by X-ray scattering [40]. As discussed in reference [34], when the system exhibits local order (induced by the micelle-micelle interaction) with a range d , one can only observe elastic behavior by probing the system on scales smaller than this correlation distance. The time τ needed to relax the stress can then be estimated as :

$$\tau \sim \frac{d^2}{6D}, \quad (3)$$

where D is the collective diffusion constant. A pictorial representation is given in figure 1 : consider a material with short-range order confined between two plates. The system can be seen as consisting of elasticity-endowed units of typical size d , the correlation distance. After applying an instantaneous shear γ by moving the upper plate to the left, one such unit (represented in thick line) has been advected from point 1 to point 2. At time $t = 0^+$ after the deformation, the stress on the upper plate is $\sigma = G_\infty \gamma$, with G_∞ the instantaneous (“infinite” frequency) shear modulus of the elastic material. Since there is no long-range restoring force, once the particles equilibrate their internal configuration (over a distance d), the elastic stress is completely relaxed; thus, after a time τ given by eq. (3), $\sigma = 0$. At $c = 50\%$, $d \sim 25 - 40$ nm and $D \sim 1.5 \cdot 10^{-10}$ m²/s, leading to a relaxation time $\tau \sim 1$ μ s. D decreases at lower concentration [44], as well as the correlation range [41], but we have no quantitative estimate for the latter. For the plateau modulus G_∞ one can take the shear modulus of the hexagonal phase, because at high frequency the structure is probed on scales smaller than the correlation length, where it is locally organized. Its value, $G_\infty \sim 5 \cdot 10^4$ Pa, is in good agreement with the experimental results. The modulus varies rapidly with the distance a between micelles ($G_\infty \sim k_B T/a^3$), so it should decrease at lower concentration.

When the system is not completely connected, both previously described processes are relevant so, in the simplest approach, we can assume that the shear modulus is a sum of two mechanisms, one related to polymer-like dynamics and the other given by order relaxation, each one with a characteristic time scale. Thus, in the first approximation we expect a bimodal relaxation of the form $G(t) = G_{\infty 1} \exp(-t/\tau_1) + G_{\infty 2} \exp(-t/\tau_2)$ or, in the frequency domain :

$$G^*(\omega) = G' + iG'' = \frac{i\omega\eta_1}{1 + i\omega\tau_1} + \frac{i\omega\eta_2}{1 + i\omega\tau_2}, \quad (4)$$

where τ_1 and τ_2 are the respective relaxation times, while G' and G'' are the storage and loss moduli, describing elasticity and dissipation, respectively. We express the complex shear modulus $G^*(\omega)$ as a function of the terminal viscosities η_1 and η_2 which can be more reliably determined from the low-frequency data than the plateau moduli $G_{\infty i} = \eta_i/\tau_i$, $i = 1, 2$. For definiteness, subscript ‘1’ will denote the slower relaxation mechanism (*i. e.* $\tau_1 > \tau_2$).

4 Results and Discussion

We performed rheology measurements in the isotropic phase of C₁₂EO₆/H₂O at different concentrations and temperatures. We present in figure 2 the values of the viscosity at

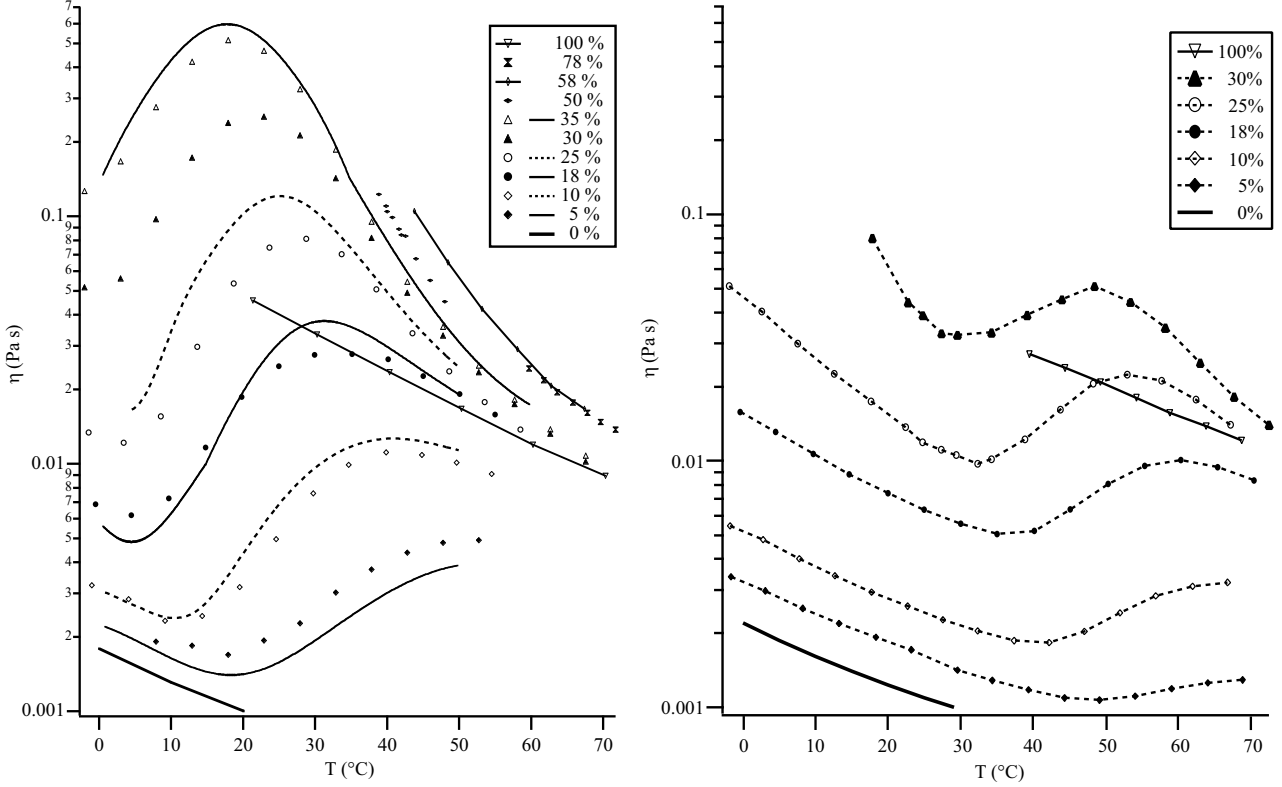


Figure 2: Left : Low frequency viscosity at different concentrations and temperatures in the isotropic phase of the $C_{12}EO_6/H_2O$ mixture (various symbols) compared to the results of Strey [36] (full and dotted lines). Right : Low frequency viscosity in the isotropic phase of the $C_{12}EO_8/D_2O$ mixture.

$\nu = 100 \text{ Hz}$ or $\omega \simeq 600 \text{ s}^{-1}$ ¹, as well as the values obtained by Strey [36] using capillary rheometry (at zero frequency) for $c \in \{5, 10, 18, 25, 35\} \%$, shown in full or dotted line. Note that at high concentration ($c \geq 50\%$ for $C_{12}EO_6/H_2O$ and $c \geq 30\%$ for $C_{12}EO_8/D_2O$) the curves stop abruptly at lower temperature because of the presence of the mesophases (see reference [35] for the phase diagrams) and of a crystalline phase for the pure surfactants. Our results are in good agreement with those of Strey, who employed a totally different technique. This validates the precision of our technique and confirms that sample concentration does not drift during the experiment. The difference $\Delta\eta = \eta(0) - \eta(600)$ between the values of Strey (at $\omega = 0$) and our results for $\omega = 600 \text{ s}^{-1}$ could be due to lower frequency relaxation mechanisms or, more probably, it only reflects the uncertainty of the measurement. We have however plotted $\Delta\eta$ for each concentration in figures 3 and 5.

The low frequency viscosity is the sum of the viscosities associated to the various relaxation mechanisms. Performing rheology measurements over a wide frequency range allows us to separate those mechanisms. We now present the frequency behavior of $G^*(\omega)$

¹At lower frequency, the data becomes noisy (especially at low concentrations), but there is no systematic variation in viscosity with respect to $\omega = 600 \text{ s}^{-1}$.

for the different concentrations.

For higher concentrations ($c = 35$ and 30%), the curves are well fitted with the sum of two Maxwell models (4). In figure 3 we show the data for $c = 35\%$: G' and G'' as a function of ω for three temperature points (8, 23 and 33°C) and the value of the fit parameters in equation (4). Equation (4) adequately describes the data for $c = 30\%$, too.

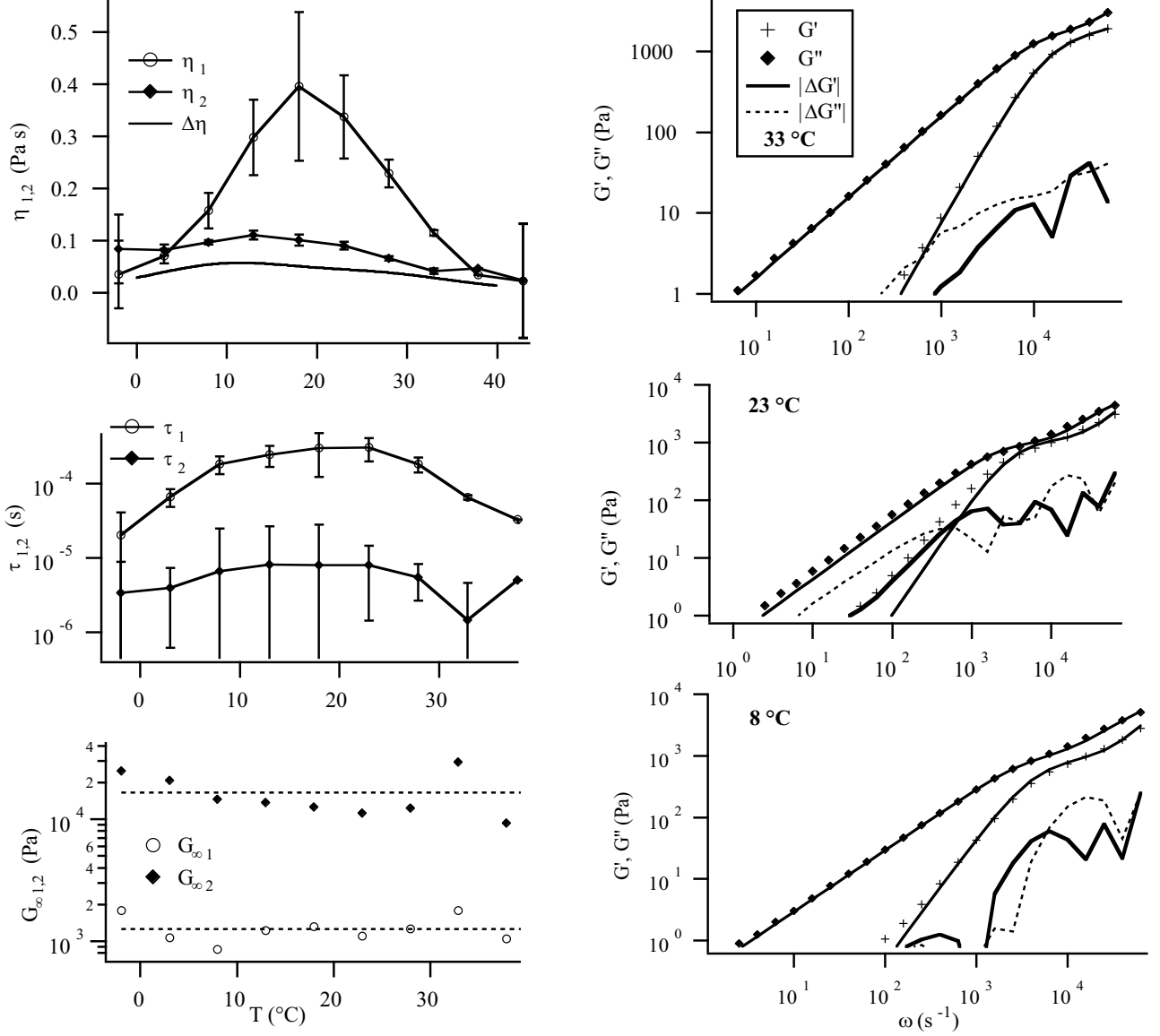


Figure 3: Rheology data for the $\text{C}_{12}\text{EO}_6/\text{H}_2\text{O}$ system at $c = 35\%$. Left : Value of the fit parameters in equation (4), as well as $G_{\infty i} = \eta_i/\tau_i$. The upper graph also shows the difference between the viscosity measured by Strey [36] (at $\omega = 0$) and our values at $\omega = 600\text{ s}^{-1}$ ($\Delta\eta = \eta(0) - \eta(600)$). Right : The value of G' and G'' as a function of ω and the corresponding fit with two Maxwell models (for 33°C , 23°C and 8°C). Thin line : fit to the data; thick line : residue of G' ; dotted line : residue of G'' .

Figure 4 shows the fit parameters. Note that τ_2 is smaller (and its values are less reliable)

than for $c = 35\%$. For $c = 18$ and 25% the fit with equation (4) yields a very small τ_2 and fit quality does not change if we set $\tau_2 = 0$ (which amounts to adding a constant viscosity background to the first Maxwell model). The fit parameters are represented in figure 5.

Finally, for the lower concentrations ($c = 5$ and 10%), no storage modulus G' is detected. The solutions exhibit simple viscous behavior and the viscosity as a function of temperature is shown in figure 2.

On the other hand, there is no sign of the slow relaxation mode for the $C_{12}EO_8/D_2O$ system; for $c \leq 25\%$ the system is purely viscous in the investigated frequency range (there is no detectable storage modulus), and the values for the low-frequency viscosity are given in figure 2 (right).

In accordance with previous results [34], we assign the fast mechanism in the $C_{12}EO_6/H_2O$ to the relaxation of local order; both the relaxation time τ_2 (in the μs range) and the plateau modulus $G_{\infty 2} \sim 2 \cdot 10^4$ Pa at $30 - 35\%$ – figures 3 and 4) are coherent with the values previously obtained for $c = 50\%$. This mechanism is also detected in the $C_{12}EO_8/D_2O$ system at $c = 30\%$; the corresponding viscosity is presented in figure 2 (right) and the relaxation time and plateau modulus (only detectable by our technique between about $40 - 55^\circ C$) are given in figure 6.

As to the slow relaxation mechanism, it is only present in the $C_{12}EO_6/H_2O$ system, with longer micelles, and it does not appear in the $C_{12}EO_8/D_2O$ solution, where the micelles are shorter. We can therefore consider that it is due to the entangled network relaxing by micellar reptation. The relaxation time τ_1 first increases with temperature, goes through a maximum and subsequently decreases. The viscosity $\eta_1 = G_{\infty 1} \tau_1$ has a similar evolution. The temperature position of the maximum goes from $18^\circ C$ at $c = 35\%$ to $35^\circ C$ at $c = 18\%$. As discussed in the theoretical section, this variation can be understood as an increase in micellar size, followed by the appearance of connections. This variation is coherent with the fact that the curvature of the aggregates diminishes with increasing temperature (due to the decreasing hydration of the nonionic polar groups [45, 46]), favoring low-curvature junctions over high-curvature end-caps. τ_1 takes values around 10^{-4} s (figures 3-5), much smaller than the usual reptation times in wormlike micellar systems [26, 24, 23]; the difference could be a sign that the entangled micelles become connected before they reach a sizeable length. An alternative explanation for this fast dynamics would be a very short breaking time τ_{br} .

The corresponding plateau modulus $G_{\infty 1}$ changes both with the concentration and the temperature. Especially at the lower concentrations (figure 5), $G_{\infty 1}$ increases with temperature, a variation which might be related to the appearance of connections or to a change in persistence length. Let us consider in more detail the concentration dependence of $G_{\infty 1}$ in the low-temperature ($15 - 20^\circ C$) range, where the micelles are not yet connected. As shown in figure 7, its variation can be described by a power law : $G_{\infty 1} \propto c^{2.6 \pm 0.1}$. For semidilute polymer solutions, this exponent can be theoretically estimated at $9/4$ but is actually slightly higher, depending on the quality of the solvent [47]. This result further reinforces our conclusion that the slower mode is due to the relaxation of the entangled network.

We would like to point out that solutions of lecithin/ H_2O/n -decane exhibit a similar bimodal relaxation spectrum (as recently shown by Schipunov and Hoffmann [19]), where the low-frequency mechanism seems to disappear upon heating (see their figure 18). Since

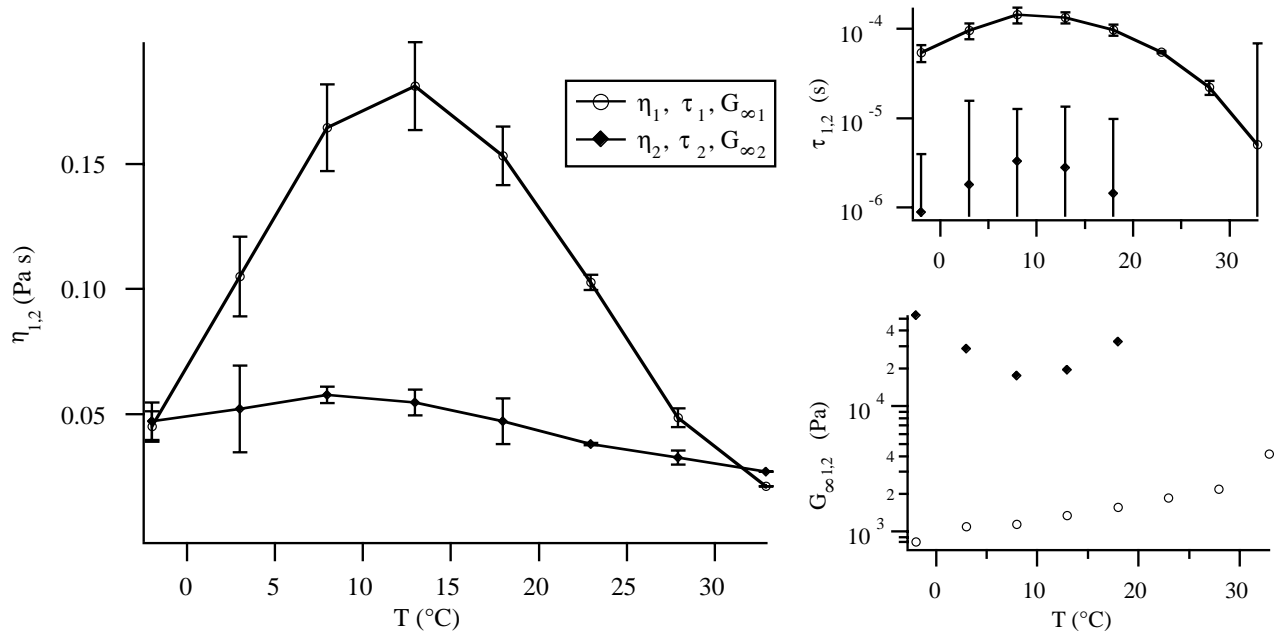
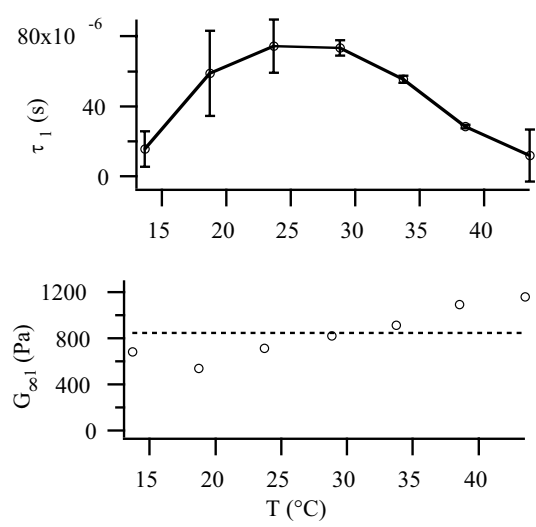
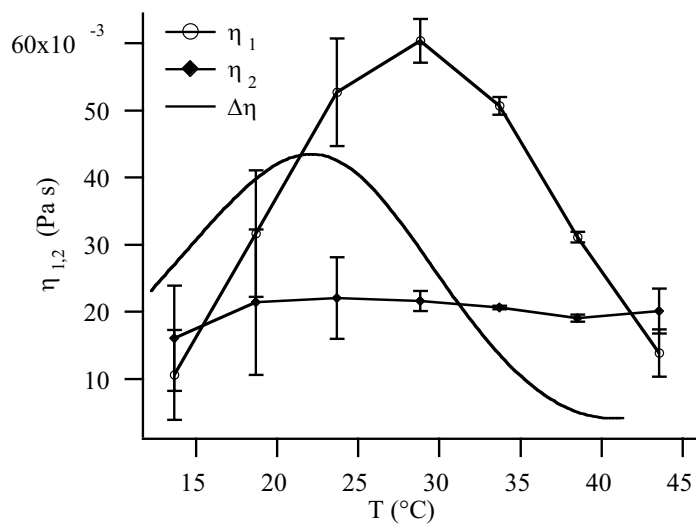
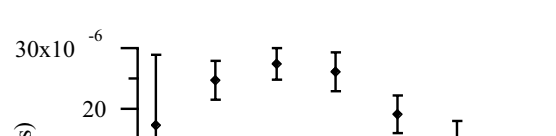


Figure 4: Rheology data for the C₁₂EO₆/H₂O system at $c = 30\%$.



10

a)



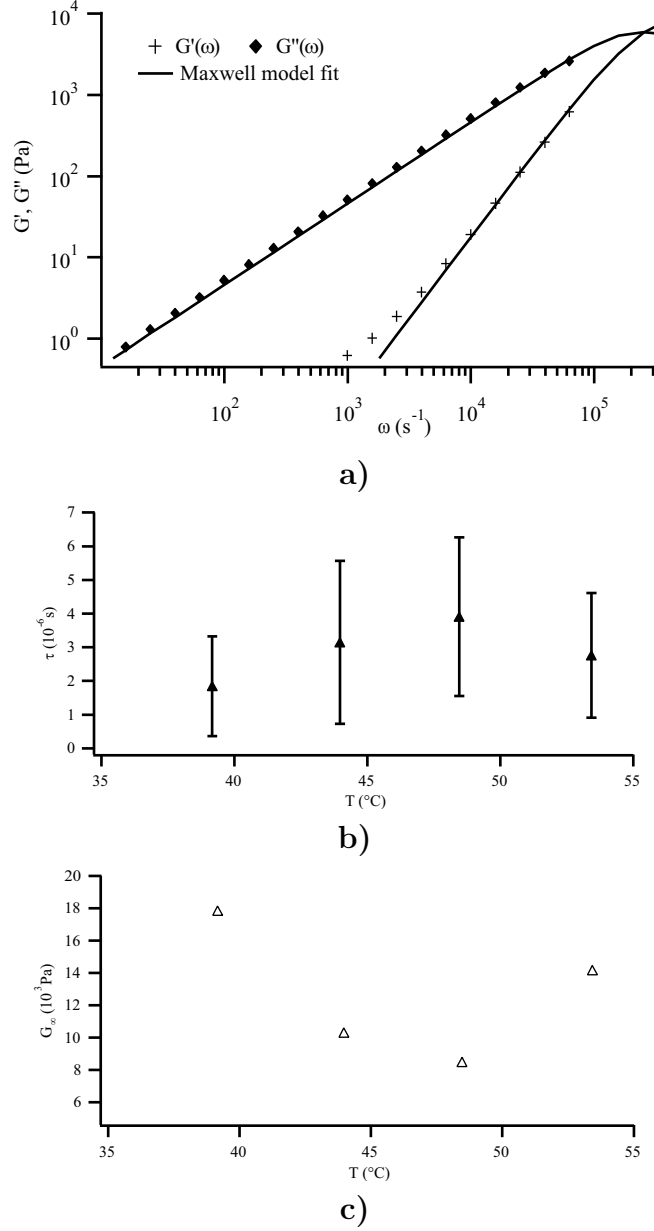


Figure 6: Rheology results for the $\text{C}_{12}\text{EO}_8/\text{D}_2\text{O}$ mixture at $c = 30\%$: a) Maxwell model fit at $T = 48.5^{\circ}\text{C}$ b) relaxation time τ and c) plateau modulus G_{∞} as a function of temperature.

these systems are very viscous and the entire relaxation spectrum is accessible to conventional rheometers, a systematic investigation of their behavior in concentration and temperature could yield interesting information, as Laplace transform techniques could be used on the rheology data in order to obtain the distribution of relaxation times $H(\tau)$ [4]. Unfortunately, we cannot apply this technique for our system because our frequency range does not cover the entire relaxation spectrum. This is why we limited ourselves to the simplest phenomenological model (two Maxwell relaxations), which is nevertheless sufficient for separating the contribution of the two physically relevant mechanisms.

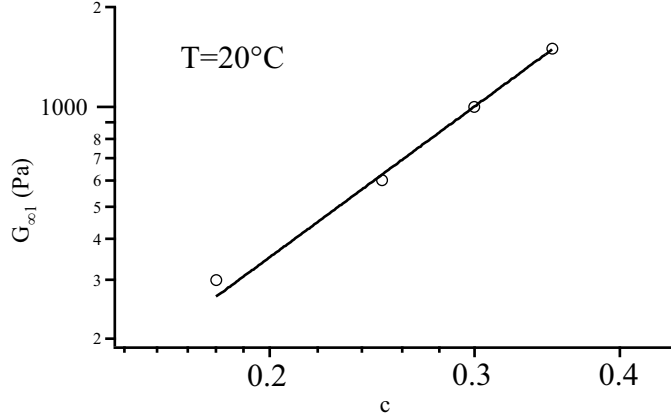


Figure 7: Plateau modulus $G_{\infty 1}$ of the slow relaxation mode in the $C_{12}EO_6/H_2O$ system at 20°C as a function of the concentration. The line is a power-law fit with exponent 2.6.

5 Conclusion

In the present work, we use high-frequency rheology to elucidate the dynamical properties of the isotropic phase in the nonionic surfactant system $C_{12}EO_6/H_2O$. We show that the relaxation spectrum can be interpreted as the sum of two mechanisms; one of them, with a relaxation time in the microsecond range, varies little in temperature and can be attributed to the relaxation in local micellar order. The second one, at about 10^{-4} s, corresponds to the relaxation of the entangled network and its temperature variation (increase, then decrease) can be explained by the micelles lengthening and then becoming connected. When the system is highly connected, only the fast mode –related to the local order– is significant. The slower mode does not appear in the $C_{12}EO_8/D_2O$ system, where the micelles are much shorter, confirming that it is related to the existence of the entangled network.

We conclude that our results show the importance of local order in concentrated isotropic surfactant phases; local order relaxation can even dominate the dynamical behaviour of the system when slower mechanisms (reptation etc.) are irrelevant. We also hope to illustrate the usefulness of high-frequency rheology for the study of surfactant solutions.

References

- [1] Lindmann, B.; Wennerström, H. *J. Phys. Chem.*, **1991**, *95*, 6053.
- [2] Ravey, J.-C. *J. Coll. Interface Sci.*, **1983**, *94*, 289.
- [3] Carale, T. R.; Blanckshtein, D. J. *J. Phys. Chem.*, **1992**, *96*, 459.
- [4] Ferry, J. D. *Viscoelastic Properties of Polymers*, 3rd ed.; John Wiley and Sons : New York 1980.

- [5] Larson, R. G. *The Structure and Rheology of Complex Fluids*; Oxford University Press : Oxford 1999.
- [6] Cates, M. E.; Candau, S. J. *J. Phys. Cond. Matt.*, **1990**, *2*, 6869.
- [7] Granek, R.; Cates, M. E. *J. Chem. Phys.*, **1992**, *96*, 4758.
- [8] Granek, R. *Langmuir*, **1994**, *10*, 1627.
- [9] Cates, M. E. *J. Phys. Cond. Matt.*, **1996**, *8*, 9167.
- [10] Lequeux, F.; Candau, S. J. “Dynamical Properties of Wormlike Micelles” in *Structure and Flow in Surfactant Solutions* (ACS Symposium Series 578) Herb, C. A.; Prud’homme R. K. eds.; ACS Books: Washington DC, 1994.
- [11] Porte, G.; Gomati, R.; El Haitamy, O.; Appell, J.; Marignan, J. *J. Phys. Chem.*, **1986**, *90*, 5746.
- [12] Ninham, B. W.; Barnes, I. S.; Hyde, S. T.; Derian, P. J.; Zemb, T. N. *Europhys. Lett.*, **1987**, *4*, 561.
- [13] Alami, E.; Kamenka, N.; Raharimihamina, A.; Zana, R. *J. Coll. Interf. Sci.*, **1993**, *158*, 342.
- [14] Kato, T.; Terao, T.; Seimiya, T. *Langmuir*, **1994**, *10*, 4468.
- [15] Kato, T.; Toguchi, N.; Terao, T.; Seimiya, T. *Langmuir*, **1995**, *11*, 4661.
- [16] Kato, T. *Progr. Colloid. Polym. Sci.*, **1996**, *100*, 15.
- [17] Mallamace, F.; Lombardo, D. *Phys. Rev. E*, **1995**, *51*, 2341.
- [18] Bernheim-Groswasser, A.; Wachtel, E.; Talmon, Y. *Langmuir*, **2000**, *16*, 4131.
- [19] Schchipunov, Yu. A.; Hoffmann, H. *Langmuir*, **1998**, *14*, 6350.
- [20] Ambrosone, L.; Angelico, R.; Ceglie, A.; Olsson, U.; Palazzo, G. *Langmuir*, **2001**, *17*, 6822.
- [21] Monduzzi, M.; Olsson, U.; Söderman, O. *Langmuir*, **1993**, *9*, 2914.
- [22] Appell, J.; Porte, G.; Khatory, A.; Kern, F.; Candau, S. J. *J. Phys. II (France)*, **1992**, *2*, 1045.
- [23] Khatory, A.; Lequeux, F.; Kern, F.; Candau, S. J. *Langmuir*, **1993**, *9*, 1456.
- [24] Narayanan, J.; Manohar, C.; Kern, F.; Lequeux, F.; Candau, S. J. *Langmuir*, **1997**, *13*, 5235.
- [25] Hassan, P. A.; Candau, S. J.; Kern, F.; Manohar, C. *Langmuir*, **1998**, *14*, 6025.
- [26] Aït Ali, A.; Makhloufi, R. *Phys. Rev. E*, **1997**, *56*, 4474.

- [27] Aït Ali, A.; Makhloufi, R. *Colloid. Polym. Sci.*, **1999**, *277*, 270.
- [28] Raghavan, S. R.; Edlund, H.; Kaler, E. W. *Langmuir*, **2002**, *18*, 1056.
- [29] May, S.; Bohbot, Y.; Ben-Shaul, A. *J. Phys. Chem. B*, **1997**, *101*, 8648.
- [30] Schmitt, V.; Lequeux, F. *Langmuir*, **1998**, *14*, 283.
- [31] Rehage, H.; Hoffmann, H. *J. Phys. Chem.*, **1988**, *92*, 4712.
- [32] Drye, T. J.; Cates, M. E. *J. Chem. Phys.*, **1992**, *96*, 1367.
- [33] Lequeux, F. *Europhys. Lett.*, **1992**, *19*, 675.
- [34] Constantin, D.; Palierne, J.-F.; Freyssingeas, E.; Oswald, P. *Europhys. Lett.*, **2002**, *58*, 236.
- [35] Mitchell, D. J.; Tiddy, G. J.; Waring, L.; Bostock, T.; McDonald M. P. *J. Chem. Soc. Faraday Trans. 1*, **1983**, *79*, 975.
- [36] Strey, R. *Ber. Bunsen-Ges. Phys. Chem.* **1996**, *100*, 182.
- [37] D'Arrigo, G.; Briganti, G. *Phys. Rev. E*, **1998**, *58*, 713.
- [38] Burnell, E. E.; Capitani, D.; Casieri, C.; Segre, A. L. *J. Phys. Chem. B*, **2000**, *104*, 8782.
- [39] Sallen, L. Ph. D. Thesis, École Normale Supérieure de Lyon, France, 1996 (Order No. 23).
- [40] Constantin, D.; Oswald, P.; Impéror-Clerc, M.; Davidson, P.; Sotta, P. *J. Phys. Chem. B*, **2001**, *105*, 668.
- [41] Zulauf, M.; Weckström, K.; Hayter, J. B.; Degiorgio, V.; Corti, M. *J. Phys. Chem.*, **1985**, *89*, 3411.
- [42] Kékicheff, P.; Nallet, F.; Richetti, P. *J. Phys. II (France)*, **1994**, *4*, 735.
- [43] Cagnon M.; Durand, G. *Phys. Rev. Lett.*, **1980**, *45*, 1418.
- [44] Brown, W.; Rymdén, R. *J. Phys. Chem.*, **1987**, *91*, 3565.
- [45] Puvvada, S.; Blanckshtein, D. J. *J. Chem. Phys.*, **1990**, *92*, 3710.
- [46] Israelachvili, J. N. *Intermolecular and Surface Forces*, 2nd ed.; Academic Press : London, 1992.
- [47] Doi, M.; Edwards, S. F. *The Theory of Polymer Dynamics*; Clarendon Press : Oxford, 1986.